Martinez-Meza *et al.*
Journal of Neuroinflammation (2025) 22:66
https://doi.org/10.1186/s12974-025-03375-w

Journal of Neuroinflammation

RESEARCH

Open Access

Antiretroviral drug therapy does not reduce neuroinflammation in an HIV-1 infection brain organoid model

Samuel Martinez-Meza[1*], Thomas A. Premeaux[2], Stefano M. Cirigliano[3], Courtney M. Friday [2], Stephanie Michael[1], Sonia Mediouni[4], Susana T. Valente[4], Lishomwa C. Ndhlovu[2], Howard A. Fine[3], Robert L. Furler O'Brien[1†] and Douglas F. Nixon[1†]

Abstract

Background HIV-1-associated neurocognitive impairment (HIV-1-NCI) is marked by ongoing and chronic neuroinflammation with loss and decline in neuronal function even when antiretroviral drug therapy (ART) successfully suppresses viral replication. Microglia, the primary reservoirs of HIV-1 in the central nervous system (CNS), play a significant role in maintaining this neuroinflammatory state. However, understanding how chronic neuroinflammation is generated and sustained by HIV-1, or impacted by ART, is difficult due to limited access to human CNS tissue.

Methods We generated an in vitro model of admixed hematopoietic progenitor cell (HPC) derived microglia embedded into embryonic stem cell (ESC) derived Brain Organoids (BO). Microglia were infected with HIV-1 prior to co-culture. Infected microglia were co-cultured with brain organoids BOs to infiltrate the BOs and establish a model for HIV-1 infection, "HIV-1 M-BO". HIV-1 M-BOs were treated with ART for variable directions. HIV-1 infection was monitored with p24 ELISA and by digital droplet PCR (ddPCR). Inflammation was measured by cytokine or p-NF-kB levels using multiplex ELISA, flow cytometry and confocal microscopy.

Results HIV-1 infected microglia could be co-cultured with BOs to create a model for "brain" HIV-1 infection. Although HIV-1 infected microglia were the initial source of pro-inflammatory cytokines, astrocytes, neurons and neural stem cells also had increased p-NF-kB levels, along with elevated CCL2 levels in the supernatant of HIV-1 M-BOs compared to Uninfected M-BOs. ART suppressed the virus to levels below the limit of detection but did not decrease neuroinflammation.

Conclusions These findings indicate that HIV-1 infected microglia are pro-inflammatory. Although ART significantly suppressed HIV-1 levels, neuronal inflammation persisted in ART-treated HIV-1 M-BOs. Together, these findings indicate that HIV-1 infection of microglia infiltrated into BOs provides a robust in vitro model to understand the impact of HIV-1 and ART on neuroinflammation.

Keywords HIV-1, Neurocognitive, Brain, Organoid, Microglia, Neurons, Neural stem cells, Inflammation, Neuroinflammation, p-NF-kB, IRIS, Antiretroviral drug therapy (ART), CCL2

[†]Robert Furler O'Brien and Douglas F. Nixon are shared senior authors.

*Correspondence:
Samuel Martinez-Meza
smartinezmeza@northwell.edu
Full list of author information is available at the end of the article

Introduction

The entry of HIV-1 into the central nervous system (CNS) occurs within 4–8 days after HIV-1-infection [1], where it infects resident macrophages, microglia, and at low levels, astrocytes [2, 3]. These infected cells respond to viral proteins, inflammatory mediators, and neurotoxic molecules by producing neuroinflammation that promotes neuronal damage and loss, that can lead to HIV-1-associated neurocognitive impairment (HIV-1-NCI) [4–6]. These neurocognitive deficits interfere with psychomotor speed and coordination, diminished memory and executive functions, and reduce the quality of life in some long-standing aviremic people living with HIV-1 (PLWH) [7–9]. Persistent chronic inflammatory changes play pivotal roles in the pathophysiology of HIV-1-NCI, which can persist even under the virological suppression provided by antiretroviral drug therapy (ART) [10].

The cause of neuroinflammation in HIV-1 infection is not fully understood and is likely multifactorial. In neurodegenerative diseases, microglia are often found near inflammatory sites like Aβ plaques, contributing to neuronal damage. In HIV-1 infection, microglia are thought to be the primary reservoir in the CNS [11–13], and may cause chronic, low-grade inflammation contributing to chronic neuroinflammation [14, 15]. Some cytokines play unique roles in the development of HIV-1-NCI. For example, CCL2 recruits immune cells, particularly those infected with HIV-1, into the CNS [16–18]. Osteopontin (OPN) contributes to the inflammatory state in HIV-1-NCI [19, 20], while TREM2, a key receptor for microglia functions, is involved in neuronal damage when cleaved into its soluble form (sTREM) [21, 22]. With ART, cytokines such as sCD14 and IL-27 are more abundant in individuals who develop Immune Reconstitution Inflammatory Syndrome (IRIS) [23, 24], which is an exaggerated inflammatory response that occurs in some PLWH after starting ART [25]. While IRIS is primarily linked to peripheral immune responses, it has recently been associated with immune-privileged organs, such as the central nervous system (CNS-IRIS), though this relationship remains poorly understood [26].

The majority of these pro-inflammatory molecules are regulated by transcription factors (TF) that control gene expression in response to pro-inflammatory stimuli. One TF that controls this expression is factor Nuclear Factor kappa-light-chain-enhancer of activated B cells (NF-kB) [27, 28]. Normally, NF-kB is kept inactive in the cytoplasm by inhibitory proteins called IκBs. When the cell is stimulated, IκB is phosphorylated by IκB kinases, leading to its degradation through ubiquitination and proteasomal breakdown [29]. The same kinases also phosphorylate NF-kB, activating it, and thus allowing it to target specific genes. In microglia, NF-kB activation is linked to neuroinflammation and brain damage, but NF-kB activity in neurons can be both protective and detrimental [30–33]. In HIV-1 infection, NF-kB activation is well-established as a key mechanism driving viral transcription in peripheral CD4 + T cells, facilitated by the translocation of p65 to the nucleus [34]. However, the role of NF-kB in CNS resident cells remains unclear. Studies utilizing postmortem brain tissue from individuals with HIV-1-NCI have demonstrated that NF-kB activation is primarily localized in perivascular microglia/macrophages and is correlated with HIV-1-associated dementia [35]. Importantly, there is no evidence of NF-kB activation in neurons in the context of HIV-1 infection. This highlights the critical need to further investigate NF-kB activation specifically within neurons in the context of HIV-1.

Access to human brain samples is limited, and animal models differ significantly from human physiology, which poses challenges for studying persistent neuroinflammation in HIV-1-NCI [36]. Therefore, there is a critical need for new technological approaches to address the study of neuroinflammation. Brain organoids (BOs) have emerged as a valuable tool to study these complexities, offering a three-dimensional differentiation of various human brain cells from stem cells [37]. A novel adaptation of the BO model involves integrating microglia that can be infected with HIV-1, thereby providing an in vitro system to investigate HIV-1-NCI [38]. This approach includes strategies, such as the infiltration of HIV-1-infected microglia into BOs [39]. However, the extent to which this model accurately reproduces the neuroinflammation characteristic of HIV-1-NCI is still being investigated. Studying how well this model mimics interactions between reactive microglia and neurons is crucial. These interactions regulate HIV-1 latency in the brain and impact HIV-1-NCI [40].

This study investigates the mechanisms of HIV-1 related neuroinflammation in a BO model that incorporates microglia and ART. This model replicates features seen in people with HIV-1-NCI, such as heightened levels of phosphorylated NF-kB and pro-inflammatory molecules. Our study is the first to demonstrate that HIV-1 infection correlates with phosphorylation of NF-kB, in the HIV-1 M-BO model, across primary CNS cell types, including microglia, astrocytes, neurons, and neural stem cells (NSCs). In addition, we can use this model to assess the impact of ART on neuroinflammation. This may further our understanding of HIV-1-NCI and potentially reveal new therapeutic targets.

Methods

Brain organoids (BOs)

NIH-registered human H1 (WA01) Embryonic Stem Cells (ESCs) were purchased from WiCell Research

Institute, Inc. and maintained in mTeSR1 medium (STEMCELL Technologies). To create BOs, human ESCs colonies at 80% confluency were plated in low-attachment 96-well plates (9000 cells per 150 µL of STEMdiff Neural Induction Medium (STEMCELL Technologies)). Embryoid bodies were fed every other day for 6–7 days, and medium containing 50mM Rho-associated protein kinase (ROCK) inhibitor was added for the first 4 days. To initiate neural rosette formation, embryoid bodies were transferred to Matrigel-coated (Corning #354277) 6-well plates where they received daily medium changes for 6–7 days. Neural rosettes were then replated a second time to increase purity for an additional 5–7 days. Following the second round of formation, neural rosette clusters were transferred to droplets of Matrigel (Corning #356234) by pipetting into cold Matrigel on a sheet of Parafilm. Droplets were solidified at 37 °C and were subsequently grown without agitation for 4 days in differentiation medium containing a 1:1 mixture of DMEM/F12 and Neurobasal, 1:200 N2 supplement (Thermo Fisher Scientific), 1:100 B27 supplement without vitamin A (Thermo Fisher Scientific), 87.5 µL of 1:100 2-mercaptoethanol, 1:4000 insulin (Sigma), 1:100 Glutamax (Thermo Fisher Scientific) and 1:200 MEM-NEAA. Following this stationary growth phase, the tissue droplets were transferred to a spinning bioreactor (orbital) shaker containing BO medium, containing differentiation medium, as described above, that was supplemented with vitamin A (Thermo Fisher Scientific).

Microglia differentiation

Human hematopoietic progenitor cells (HPCs) were obtained from Children's Hospital of Philadelphia of the University of Pennsylvania (Philadelphia, PA). These HPC were derived from an iPSC line (CHOPWT6). Approximately 0.1×10^6 HPC were seeded into a 48 well plate and differentiated in Microglia medium composed of RPMI with 10% FBS, 1% penicillin/streptomycin, 1% 1M HEPES supplemented with 25ng/mL CSF-1 (Peprotech), 100ng/mL IL-34 (R&D), and 50ng/mL TGF-β (Peprotech). Half medium changes were performed every 2 days for 11 days [41].

HIV-1 infection of microglia

The differentiated cells were incubated with HIV-1 ADA a multiplicity of infection (MOI) of 0.55 in Microglia medium for 24h. The cells were washed 3 times and incubated for an additional 48h in Microglia media. "Uninfected cells" had the equivalent amount of PBS following the same protocol of infected cells.

Co-culture of microglia and brain organoids

200,000 Microglia cells in 48 well plates were either uninfected or infected with HIV-1 (labeled or unlabeled), washed, and microglia media replaced with 500µL BO media. One BO was added to each well, and the plates were incubated at 37 °C for 24 h with no orbital shaker. Subsequently, the organoids were flipped and left undisturbed for an additional 24 h to maximize contact. Each organoid was then washed in PBS 3 times and transferred to a clean well (Day 0) with 2mL BO medium alone or supplemented with ART (Nelfinavir and Raltegravir both at 1mM) as applicable (ART interruption was with supplementation of ART for only 12 days). BOs with infiltrated Microglia were maintained on an orbital shaker for up to 25 days at 37 °C. After 25 days, BOs were cut into two equal pieces. One was analyzed for inflammation markers and the presence of HIV-1, while the other was embedded in paraffin for microscopic analyses.

Labeled microglia

Microglia were detached from the flasks and incubated with 1nM tracking dye Celltracker Orange (Thermofisher #C2927) for 20 min in media without serum at 37 °C or without cell tracker for unlabeled control cells. The cells were washed 3 times with media without serum and resuspended in microglia media at 1×10^6 cells/ml. 200 µl of resuspended cells was seeded in 48 plates for 24 h.

Flow cytometry of BOs

BOs were incubated with 20nM calyculin A (cell signaling #9902), a phosphatase inhibitor, for 10 min before processing. Subsequently, half of each BO was dissociated using a papain dissociation kit (Worthingthon #LK003150), with a 30-min papain incubation supplemented with calyculin A. Following papain inactivation as per the manufacturer's protocol, the cells were collected, distributed into staining flow cytometry tubes, and kept on ice. For microglia cultures, cells were detached using a Trypsin/EDTA mix; uninfected cells were treated for 5 min and HIV-1 infected cells for 15 min at 37 °C. The cells were then washed and centrifuged twice at 1800 rpm for 5 min at 4 °C using a staining buffer (PBS with 2% BSA). The cells were finally resuspended in PBS and incubated for 15 min with either 4nM DAPI or 1nM Live/Dead fixable Aqua cell stain (Thermo Fisher # L34957) to label dead cells. The microglia cells were washed three times with staining buffer and incubated with surface antibodies CD45 (BD #563792), CD11b (BD#564517), P2RY12 (Biolegend #392106), and TREM2 (R&D FAB17291A) for 40 min. The FIX/PERM Kit was employed for intracellular staining with antibodies against IBA-1(Cell Signaling #78060S), TUJ-1(ab195879),

Pax6 (Milteny Biotech #130123267), Sox2(Milteny Biotech #130120721), p65 p-NF-κB at Ser536 (Cell Signaling #5733), and GFAP (Cell Signaling #3655S). Labeled cells were fixed with 2% paraformaldehyde in 1% BSA/PBS and analyzed using an Attune NxT flow cytometer (ThermoFisher Scientific).

Soluble marker quantification

Stored supernatants from HIV-1 infected, uninfected IPSC-derived microglia cultured 3 days post-infection, and all M-BOs conditions at days 3, 9, 18, and 25 days of culture were tested. M-BO supernatants were concentrated fivefold using Pierce protein concentrators (50K MWCO, Thermo Fisher Scientific). The following cytokines and chemokines were evaluated using a custom multiplex immunoassay (R&D systems): Soluble CD14 (sCD14), soluble CD163 (sCD163), MCP-1(CCL2), CCL19/MIP-3b, CX3CL1/Fractalkine, Interferon-γ (IFNγ), Interleukin-1 beta (IL-1β), IL-6, IL-10, IL-27, Osteopontin/SPP1 (OPN), Soluble TREM2 (sTREM2), and Tumor necrosis factor-α (TNFa). Data was acquired on a Luminex IntelliFLEX system (Luminex) and analyzed using MILLIPLEX® Analyst software (Millipore). All samples were analyzed in duplicate.

Immunofluorescence

To monitor the infiltration of microglia-labeled cells into the organoids, we captured images of the entire BO using the fluorescence microscope Keyence BZ-X800E with a CY3 filter at various days of incubation. For the analysis of other cell populations and phosphorylation levels, the BOs were fixed and permeabilized. Subsequently, they were embedded in paraffin, and slides were prepared by the Histowiz company for further examination. Before initiating the staining protocol, the slides underwent deparaffinization and rehydration, including 10 min in Cytrosolv (×2), 2 min in 100% ethanol (×2), 2 min in 95% ethanol, 2 min in 70% ethanol, and 2 min in PBS (×2). Subsequently, heat-induced epitope retrieval (HIER) was conducted in a water bath 92–95 °C for 15 min and submerged in Trilogy solution (Cell Marque). Another container with Trilogy was heated, and the sections were transferred for an additional 5 min. Permeabilization (required for nuclear antigens) was carried out for 20 min with PBS/0.5% Triton-X-100 at room temperature, followed by immersing the slides in PBS for 5 min. Sections were incubated for 1 h with PBS/3% BSA (approximately 200 µl per section) to block nonspecific staining. The antibody was diluted in 3% BSA in PBS at different dilutions: Tuj-1(AB 195879) 1/100, anti-p-NF-kB (Cell signaling #5736) 1/50, MAP2 (AB225316) 1/100, Olig2 (Cell Signaling #65915T) 1/250, Nestin (Cell signaling #33475S)1/400, CCl2 (R&D IC279G)1/50, S100B (Milipore #S2532) 1/250 dilution, anti-mouse incubated overnight at 4 °C. Slides were washed three times for 5 min each in PBS with gentle agitation. Sec antibody 1/200 (Life technology #R6393) and anti-rabbit Sec antibody 1/200 (Life technology #A11008) were incubated for 1 h in 3% BSA in PBS. Finally, they were mounted with an anti-fade mounting media with DAPI and visualized using fluorescence and confocal microscopy.

ddPCR assay

DNA extraction from M-BOs from experimental treatment conditions: Uninfected, HIV-1, HIV-1 + ART, and HIV-1 + ART Interrupted, was performed using the QIAamp DNA/RNA Mini Kit (Qiagen) and incorporated precautions to minimize DNA shearing. The HIV-1 and human RPP30 reactions were conducted independently in parallel, and the resulting copy numbers were normalized based on the quantity of input DNA. Each ddPCR reaction was performed with ddPCR Supermix for Probes (no dUTPs, BioRad), primers (final concentration 900 nM, Integrated DNA Technologies), probes (final concentration 250 nM, ThermoFisher Scientific), and nuclease-free water. A median of 7.5 ng (IQR 7–7.5 ng) of genomic DNA for RPP30 or a median of 750ng (IQR 700–750ng) for HIV-1 was used. The primer and probe sequences (5′–>3′) used were as follows: RPP30 Forward Primer: GATTTGGACCTGCGAGCG, RPP30 Reverse Primer: GCGGCTGTCTCCACAAGT, RPP30 Probe: VIC-CTGACCTGAAGGCTCT-MGBNFQ; HIV-1 Ψ Forward Primer: CAGGACTCGGCTTGCTGAAG, HIV-1 Ψ Reverse Primer: GCACCCATCTCTCTCCTTCTAGC, HIV-1 Ψ Probe: FAM-TTTTGGCGTACTCACCAGT- MGBNFQ. Droplets were generated using the Automated or QX200 Droplet Generator (BioRad) and subjected to cycling at 95 °C for 10 min. This was followed by 45 cycles of 94 °C for 30 s, 59 °C for 1 min, and 98 °C for 10 min. Droplet analysis was performed on a QX200 Droplet Reader (BioRad) using QuantaSoft software (BioRad, version 1.7.4). Fluorescence thresholds were set above the levels detected in both negative controls and no-sample wells for each experiment. Droplets with fluorescence above this threshold were classified as positive, while those below were classified as negative. Positive droplets were automatically analyzed by QuantaSoft software and converted into copies per microliter (copies/µL) of the target sequence. The number of HIV-1 copies per million cells was calculated based on the estimated cell count; assuming two copies per cell, the number of RPP30 copies was divided by two.

Statistics

Differences in supernatant biomarkers levels between uninfected and HIV-1 infected microglia were

determined by the Mann Whitney test. Soluble marker differences among M-BO infection and ART treatment groups and time points were determined by two-way ANOVA adjusted for multiple comparisons (Tukey test). Differences in population and p-NF-kB levels detected by flow cytometry were determined by one-way ANOVA adjusted for multiple comparisons (Tukey test). All BOs used in this study were from the same organoid batch, with each organoid treated as an independent experiment, and is represented by a single point in the graphs.

Results

BOs and microglia show an inflammatory response in response to pro-Inflammatory stimuli associated with HIV-1 infection

BOs provides a comprehensive approach to understanding interactions between different CNS cell types in specific pathologies, including HIV-1-NCI [38, 42, 43]. The creation of BOs is a complex process that begins with deriving cells from ESCs. These cells self-organize to form distinct brain regions within a three-dimensional structure [44]. Human ESCs were differentiated into BOs according to the protocol previously described [45]. A typical signature of differentiation activity inside BOs is the formation of rosette structures. These structures are apico-basally polarized, stratified, flower-like formations that NSCs create in vitro during the differentiation into different cell types such as neurons, oligodendrocytes, and astrocytes [46]. The H&E staining of BOs reveals the presence of several rosette structures in the BOs as a sign of active development (Fig. 1A). Magnification of these structures allows identification of different layers of differentiation, from NSCs in the lumen to the mature neurons towards the apical side. In addition to the magnified

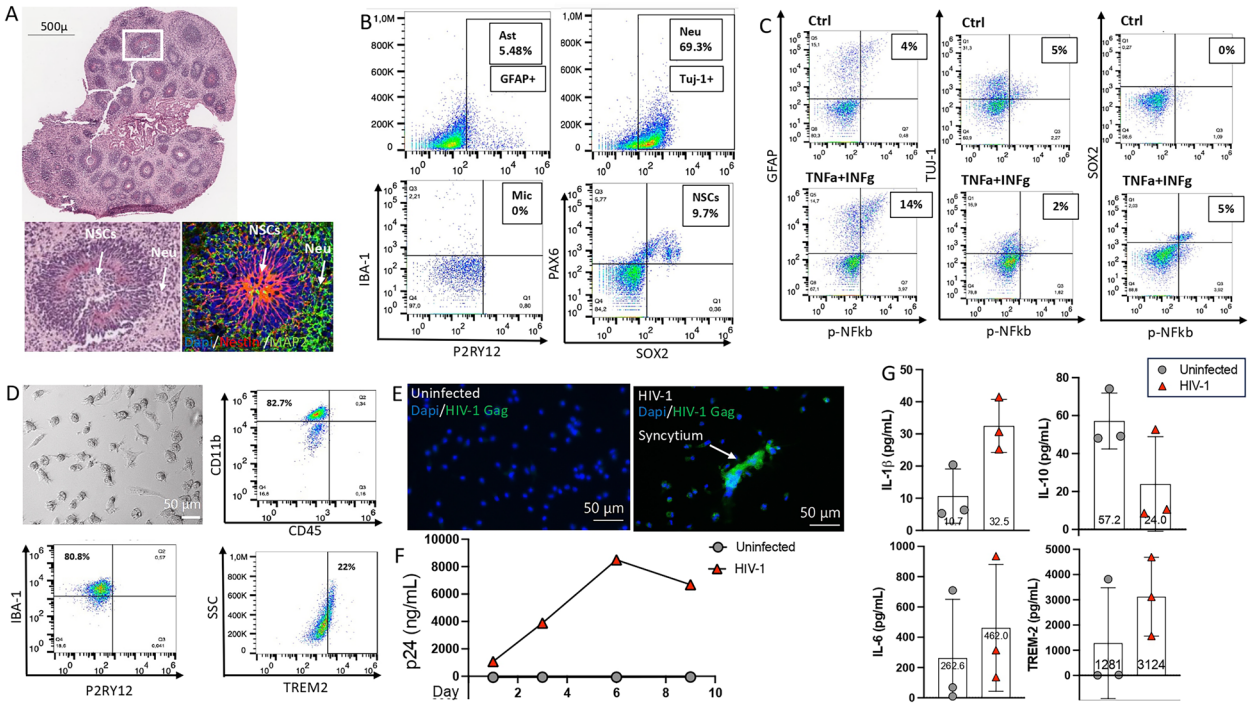

Fig. 1 Characterization of mature microglia and BO morphology in response to pro-inflammatory stimuli. **A** H&E staining of 4-month-old BO. The image shows typical BO morphology with classical rosette structures. The magnified section indicates the location of neuro stem cells (NSCs) and mature neurons (Neu) within the rosette structure. The immunofluorescence of the rosette structure confirm the presence of NSCs (Nestin) and Neu (MAP2) **B** Characterization of one BO by obtained by flow cytometry analysis, identifying different populations: 5.48% GFAP + reactive astrocytes (Ast), 69.3% Tuj-1 + neurons (Neu), 0% Iba-1 + /P2RY12 + microglia (Mic), and 9.7% PAX6 + /SOX2 + neuro NSCs. **C** p-NF-KB levels in one BO (n = 1) stimulated with TNFa 40 ng/ml + 100ng/ml IFN in presence of 100 nM calyculin versus a BO treated with vehicle (DMSO) for 1 h, obtained by flow cytometry analysis. The dot plot shows the changes of p-NF-κB in the different BOs population characterized by CNS markers: GFAP + (reactive astrocyte), TUJ-1 (neurons) and SOX2 + (neuro NSCs). **D** Characterization of fully differentiated microglia (HPCs -derived microglia) after 11 days shows typical microglial morphology. Representative flow cytometry dot plot showing the expression of classical microglial markers: CD11b (82.7%), CD45 (low), Iba-1 (80.8%), P2RY12 (low), and TREM2 (22%). **E** Analysis of Gag expression in HIV-1 infected microglia by immunofluorescence 24 h post-infection (top images). The arrows in the images indicate syncytia structures with high Gag protein expression, characteristic of HIV-1 infection (n = 1). **F** Quantification of levels of p24 detected in the supernatant of HIV-1 infected microglia by ELISA over 9 days of incubation (graph) (n = 1) **G** Quantification of pro-inflammatory cytokine levels associated with HIV-1-NCI and IRIS in the supernatant of three different microglia batches at day 3 post-infection (n = 3)

images, we confirmed the cellular composition of the rosette structures with immunofluorescence, showing the expression of Nestin and MAP2 as classical markers for NSCs and mature neurons, respectively.

To characterize BOs, we dissociated them and analyzed their populations using flow cytometry with classic CNS markers: IBA-1 and P2R2Y for microglia, TUJ-1 for neurons, Pax6 and Sox2 for NSCs, and GFAP for astrocytes (Fig. 1B). All the populations were identified except for microglia. The absence of microglia in this BOs corroborates what had been described previously [45]. The gating strategy is detailed in (Fig S1). The oligodendrocyte population was assessed through immunofluorescence staining for Olig2 expression, alongside the astrocyte population, which was re-evaluated using immunofluorescence for GFAP and S100B expression (Fig S2).

To evaluate BOs as an in vitro model of neuroinflammation in the context of HIV-1 infection, we first assessed their inflammatory response to a pro-inflammatory stimulus. We measured the p-NF-kB in response to TNFa and IFNg: classical cytokines associated with HIV-1 infection. Flow cytometry analyses revealed that astrocyte (GFAP+) and NSCs (Sox2+) became more p-NF-kB positive after treatment, in comparison with the control, while the neuron population (TUJ-1+) became less p-NF-kB positive (Fig. 1C). The gating strategy is detailed in (Fig S3). The enhanced p-NF-kB following TNFa and IFNg stimulation support the hypothesis that BOs are capable of replicating a neuroinflammatory response in the pro-inflammatory environment generated by HIV-1-infected microglia.

To obtain microglia, we used a well-established protocol of differentiation, which involves culturing human microglia from induced HPCs [41]. Microglia were characterized after 11 days of HPC differentiation. Uninfected microglia displayed a morphology consistent with previous studies and expressed well-established microglia markers (Fig. 1D). We showed a pattern of expression characterized by an 82.7% of CD11b+/CD45low, 80.8% IBA-1+, and 22% TREM2+(Fig. 1A). The gating strategy is detailed in (Fig S4). Microglia were infected with HIV-1, as evidenced by syncytium formation in HIV-1 and the elevated presence of Gag by immunofluorescence 48 h post-infection (Fig. 1E). The supernatant of HIV-1 infected and uninfected microglia cultures was measured by ELISA during a 9-day incubation period. The detection of p24 in HIV-1 infected microglia, in contrast to uninfected microglia, confirmed successful HIV-1 infection. The levels of p24 increased until day 6 before experiencing a decline (Fig. 1F). Since microglia are a key source of neuroinflammation, we assessed their role in the inflammatory response. We measured pro-inflammatory cytokine levels after 3 days of HIV-1 infection. A panel of 11 cytokines was selected, including those associated with HIV-1-NCI such as CCL-2, Fractalkine, IFN-g, IL-1b, IL-6, IL-10, IL-27, OPN, sTREM2, and TNFa. Additionally, two cytokines linked to inflammation associated with antiretroviral therapy IRIS, such as IL-27 and soluble sCD14 [23, 24], were included. See (Table 1) for more details.

Only eight cytokines from the panel were detected in the microglia supernatants, and some of them showed increased levels of pro-inflammatory cytokines in the infected microglia. Pro-inflammatory cytokines such as IL-1(from 10.67 ± 8.443 to 32.48 ± 8.239,$p = 0.1$), IL-6 (from 262.6 ± 388.1 to 462.0 ± 419.5, $p = 0.4$), and sTREM2 (from 1281 ± 2197 to 3124 ± 1563, $p = 0.4$) increased after infection while the anti-inflammatory cytokine IL-10 decreased (from 57.15 ± 14.75 to 23.95 ± 24.88, $p = 0.4$). Although, these changes were not statistically significant the trend observed is consistent with activation of microglia in response to HIV-1 infection (Fig. 1G). There were no differences in the other cytokines (IL-27, sCD14, sCD163 and OPN) (Fig S5). Since BOs respond to pro-inflammatory stimuli and microglia can mount a pro-inflammatory response to HIV-1 infection, we next investigated whether HIV-1 infected microglia could induce neuroinflammation in BOs.

HIV-1 infected microglia induce neuroinflammation in BOs

Various strategies have been used to introduce microglia into BOs to study brain development and related pathologies [39], including infusing exogenous HIV-1 infected microglia into BOs [38]. Here, we used microglia infiltration, and cocultured differentiated microglia with BOs [47]. A schematic outlining the experimental procedure illustrates the generation of M-BOs, starting with the differentiation of microglia (Fig. 2A). Both uninfected and HIV-1 infected microglia were infiltrated into BOs to create M-BOs: Uninfected (Uninfected M-BO) and HIV-1 infected (HIV-1 M-BO), respectively. A key aspect of HIV-1-NCI is that although ART reduces viral replication in PLWH, it does not completely alleviate high levels of inflammation in the nervous system [48] For this reason, we evaluated the impact of ART on viral replication [23–26].

A subset of HIV-1 M-BO were subjected to either continuous (M-BO HIV-1+ART) or interrupted (M-BO HIV-1+ART Interrupted) ART regimens. During all the incubations supernatant was saved to evaluate how pro-inflammatory cytokines associated with HIV-1-NCI and viral proteins change under these different conditions. After day 25, the M-BO was divided into two equal parts. One half was dissociated into single cells to confirm the presence of virus. The impact of HIV-1 and ART on different CNS populations was assessed using flow

Table 1 Cytokine panel measured by multiplex ELISA in the supernatants of microglia and M-BO cultures

Cytokine	Association with HIV-1	Reference	Microglia HIV-1 infected sup	HIV-1 M-BOs infected sup
Interleukin-1 beta (IL-1b)	Associated HIV-1-NCI through Ferritin Heavy Chain	[83, 84]	Detectable	Detectable
Tumor necrosis factor (TNFa)	Pro-inflammatory cytokines inducing neuronal death	[84]	Undetectable	Undetectable
Interferon-gamma(IFNg)	Correlate with HIV-1- NCI in PLWH. Enhance replication HIV-1 in astrocytes	[85, 86]	Undetectable	Undetectable
soluble CD163 (sCD163)	Plasma correlates with postmortem HIV-1- NCI	[48, 49]	Detectable	Detectable
IL-6	Implicated in HIV-1 neurotoxicity from human astrocytes	[87]	Detectable	Undetectable
MCP-1(CCL2)	Increase in CSF in PLWH with HIV-1-NCI Increased infiltration of HIV-1 infected cells to the CNS	[18, 70]	Undetectable	Detectable
Osteopontin/SPP1(OPN)	Increase in CSF of PLWH with HIV1-NCI. Enhances HIV-1 replication in the brain. Activation of inflammasome and recruitment of immune cells	[19, 88]	Detectable	Detectable
Soluble TREM2 (sTREM2)	Increased in CSF of PLWH with HIV-1-NCI	[21, 22]	Detectable	Undetectable
CX3CL1/Fractalkine	Protective role preventing replication of HIV-1 and inflammation	[89]	Undetectable	Undetectable
Soluble CD14 (sCD14)	Elevated plasma levels (Not CSF) correlated with poor prognosis in HIV-1 Associated with Immune reconstitution inflammatory syndrome (IRIS)	[23, 24]	Detectable	Detectable
IL-27	Potent inhibitor of HIV- 1 replication in peripheral blood Associated with IRIS	[23]	Detectable	Detectable
CCL19/MIP-3b	Increases HIV-1 infection, integration, and latency in resting CD4 + T cells Associated with CNS lymphoma	[90, 91]	Undetectable	Undetectable
IL-10	Inhibits pro- inflammatory response. Pro- inflammatory and anti- inflammatory activities in the pathogenesis of HIV-1/AIDS with meningitis. Associated with IRIS	[92]	Detectable	Undetectable

This table outlines the association of each cytokine with HIV-1-related neuropathology and indicates whether each cytokine was detected in the supernatant of microglia cultures versus M-BO cultures. Values below the LLOD (lower limit of detection) of this multiplex assay were considered undetectable

cytometry. The other half was embedded in paraffin for immunofluorescence analysis (Fig. 2A).

Successful infiltration of microglia in M-BOs was confirmed by co-culturing an additional group of M-BOs with microglia labeled with the cell tracker orange. Microscopy images revealed clusters of orange cells 5 days after microglia infiltration (Fig. 2B, Top and middle panel). No such clusters were observed in the control: BOs not infiltrated with labeled microglia (Fig. 2B, bottom panel). Flow cytometry analyses of these M-BOs showed a population labeled with cell tracker orange and positive for the microglia markers P2RY2 and IBA-1, accounting for 10% of the total cells analyzed (Fig. 2C). We used IBA-1 to identify microglia in BOs across all conditions. Positive IBA-1 populations were found in M-BOs, indicating successful integration in all conditions (Fig. 2D). Gating strategy Fig S6. Although there were significant differences between Uninfected and HIV-1 + ART (7.558 ± 0.2711 vs 10.09 ± 1.641, $p = 0.018$), the variations between all conditions were minimal (8–10%).

Confirmation of virus infection in M-BOs was performed by ddPCR (Fig. 2E). While there was a tendency towards lower copy numbers in the HIV-1 M-BO + ART Interrupted group (3123 ± 2957, $p = 0.23$), the high variability in the number of copies made it challenging to identify significant differences, as indicated by the coefficients of variability: HIV (100.4%), HIV + ART (94.7%), and HIV + ART Interrupted (89.8%). However, these results did confirm the presence of HIV-1 in the M-BOs infiltrated with HIV-1 infected microglia after 25 days of incubation.

To determine whether infiltration of HIV-1-infected microglia generated a persistent HIV-1 infection during the incubation, the supernatant from the two M-BOs with the higher psi-gag copies/10^6 cells per group was analyzed. The levels of p24 in the supernatant collected during the 25 days of incubation confirmed HIV-1 infection in M-BO HIV-1, while it was undetectable in uninfected M-BOs (Fig. 2F). The level of p24 detected corresponded with the number of copies. During the 25 days of culture, p24 levels were lower in the groups treated with ART. There was no detectable spontaneous reactivation of HIV-1 (p24 rebound) observed in the HIV-1 + ART Interrupted group (Fig. 2F), suggesting the need for additional factors to activate HIV-1 replication.

Next, we hypothesized that HIV-1-infected microglia could induce a pro-inflammatory state in the BOs. We analyzed the same panel of pro-inflammatory cytokines previously measured in the supernatant of infected microglia, but this time in the supernatants collected from M-BOs during the whole incubation period (25 days). Interestingly, only five of the eight cytokines detected in microglia, found in the supernatant

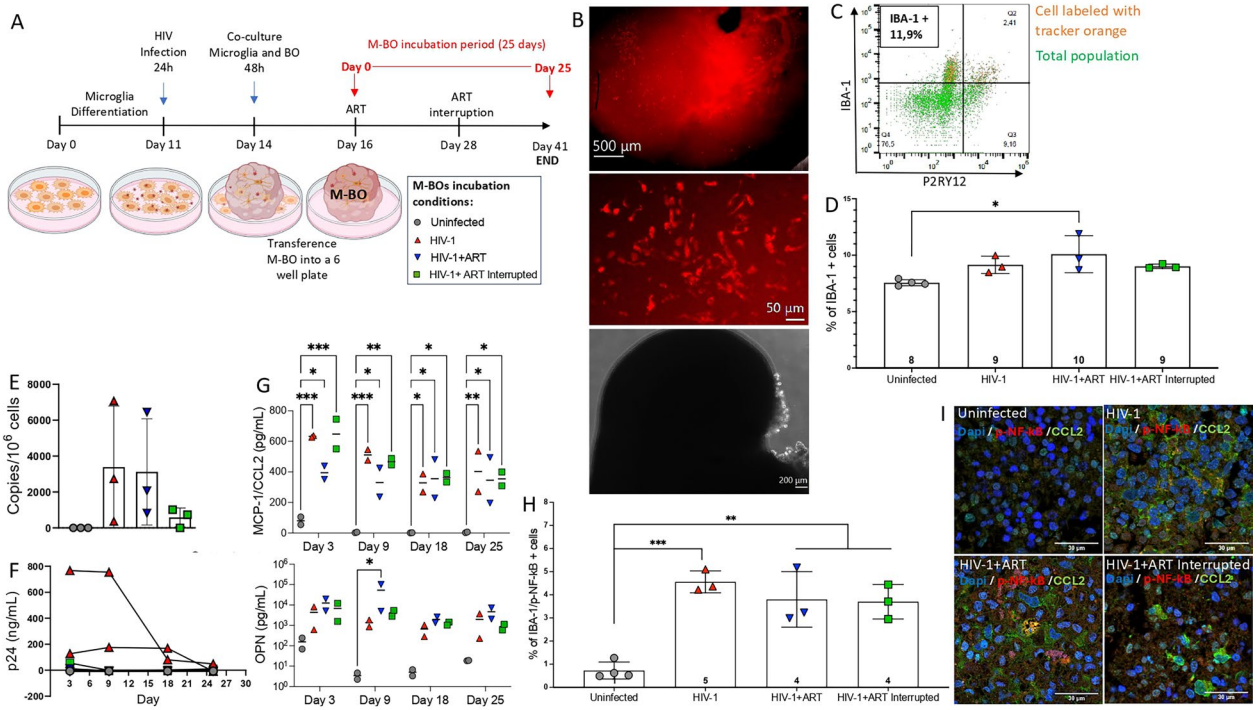

Fig. 2 HIV-1-infected microglia infiltrate BOs and promote an inflammatory response associated with HIV-1-NCI. **A** Breakdown of the experimental design, including differentiation of microglia, infection with HIV-1, co-culture with mature BOs to obtain M-BOs, experimental treatment conditions: Uninfected, HIV-1, HIV-1 + ART, and HIV-1 + ART Interrupted. **B** Image showing cluster of microglia cells labeled with cell tracker orange inside the M-BO 5 days post-co-culture captured by microscopy (top panel) and a magnification of labeled cells cluster in a different M-BO (middle panel). M-BO not infiltrated with labeled microglia as a ctrl of fluorescence signal (bottom panel) **C** Dot plot showing the percentage of orange cells detected (orange dots) IBA-1 and P2RY12 positive (n = 1) detected by flow cytometry analysis. **D** The graph displays the percentage of cells in M-BOs in the four treatment conditions positive for IBA-1 detected by flow cytometry analysis. **E** Graph of ddPCR analysis of BOs in the four treatment conditions, showing detected copies of HIV-1 psi-gag per 10^6 cells. **F** Quantification of p24 levels detected in the supernatant of M-BOs in the four treatment conditions over 25 days of incubation. Each curve corresponds to one M-BO, with two M-BOs per condition evaluated (n = 2) **G** Quantification of pro-inflammatory cytokines detected in the supernatant of M-BOs for the four treatment conditions performed in the experiment. Two M-BOs per condition were evaluated (n = 2). **H** Quantification of the percentage of double positive cells for IBA-1 and p-NF-kB in M-BOs after 25 days of incubation. **I** Immunofluorescent staining for Dapi (blue), p-NF-KB (red) and CCL2 (green), on slides of M-BOs in the 4 treatment conditions. Each organoid treated is an independent experiment and is represented by a single point in the graphs for the four treatment conditions: Uninfected (n = 4), HIV-1 (n = 3), HIV-1 + ART (n = 3), and HIV-1 + ART Interrupted (n = 3). *p ≤ 0.05, **p ≤ 0.01, ***p ≤ 0.001

of M-BOs, were different (See Table 1). Among the cytokines detected, IL-1b showed no differences across conditions, but a decrease over time was observed with sCD163 (Fig. S7). This is consistent with studies that show elevated sCD163 in the plasma but not in the cerebrospinal fluid (CSF) of people with HIV-1-NCI [49]. The cytokine sCD14 initially showed high levels in the HIV-1 M-BO group but decreased over time. In contrast, IL-27 remained low throughout the incubation period until day 25, when it increased significantly (Fig. S7).

Notably, CCL-2 and OPN levels remained low in uninfected M-BOs, while they were elevated in all HIV-1-infected M-BOs, regardless of ART treatment. While the difference in CCL-2 levels was statistically significant among all groups and time points, OPN showed significant differences only at day 9 in HIV-1 + ART M-BOs (53,347 ± 6838, p = 0.03). These observations recapitulate the persistent inflammation observed in PLWH with HIV-1-NCI on ART (Fig. 2G).

The pro-inflammatory profile shown by our model under different conditions suggests a key role for these cytokines in maintaining persistent neuroinflammation associated with HIV-1. Therefore, we measured p-NF-kB in microglia found in M-BOs to evaluate their contribution to neuroinflammation. Notably, microglia had significantly higher p-NF-kB levels in M-BOs infiltrated with HIV-1 infected microglia compared to uninfected microglia, irrespective of the ART regimen (Fig. 2H). This correlated with the levels of CCL2 and OPN detected previously. Although CCL2, a pro-inflammatory cytokine, has been shown to be regulated by NF-kB in other pathological conditions [50, 51], including astrocyte activation in injury contexts [52], it has not yet been explored in the context of neuro-HIV-1. A

double-staining immunofluorescence for CCL-2 and p-NF-kB among all conditions showed a correlation between CCL-2 expression and elevated p-NF-kB levels in all HIV-1-infected conditions, regardless of ART, suggesting a link between p-NF-kB activation and CCL-2 expression (Fig. 2I). These results support the characteristic ART-resistant neuroinflammation observed in PLWH with HIV-1-NCI.

Although microglia are one of the main sources of pro-inflammatory cytokines in the CNS, other cell types are important for neuroinflammation. We investigated how other cell populations in the M-BOs, such as astrocytes, neurons and NSCs, were affected by the infiltration of HIV-1-infected microglia and the administration of ART.

The neuroinflammation induced by HIV-1 infected microglia in BOs correlated with an increase of astrocyte reactivation and NF-kB activation in an ART-independent manner

Astrocytes are among the most critical CNS cell populations driving neuroinflammation [53]. In the context of HIV-1 neuropathology, it has been shown that astrocytes become reactive and contribute to astrogliosis [54, 55]. Although only a small percentage of astrocytes appear to be directly infected by HIV-1, they are now considered a functional reservoir for the virus [56]. Given the recognized role of astrocytes in HIV-1-NCI, we examined their response to HIV-1 infection.

To assess astrocyte presence and reactivity, we measured levels of GFAP, a classical marker of reactive astrocytes, in combination with p-NF-kB. GFAP staining revealed a consistent astrocyte population across all conditions, with the exception of the uninfected control where GFAP expression was absent (Fig. 3A, B). Immunofluorescence analysis further confirmed this finding, showing a similar pattern using GFAP and additional marker of astrocyte, S100B (Fig. 3C). Additionally, we analyzed p-NF-kB levels (Fig. 3D), revealing a significant increase in a consistent population double-positive for GFAP and p-NF-kB in all HIV-1-infected conditions, similar to what was observed in the microglia population. These results confirm that astrocytes respond to HIV-1 presence with a proinflammatory state, characterized by elevated expression of GFAP and p-NF-kB.

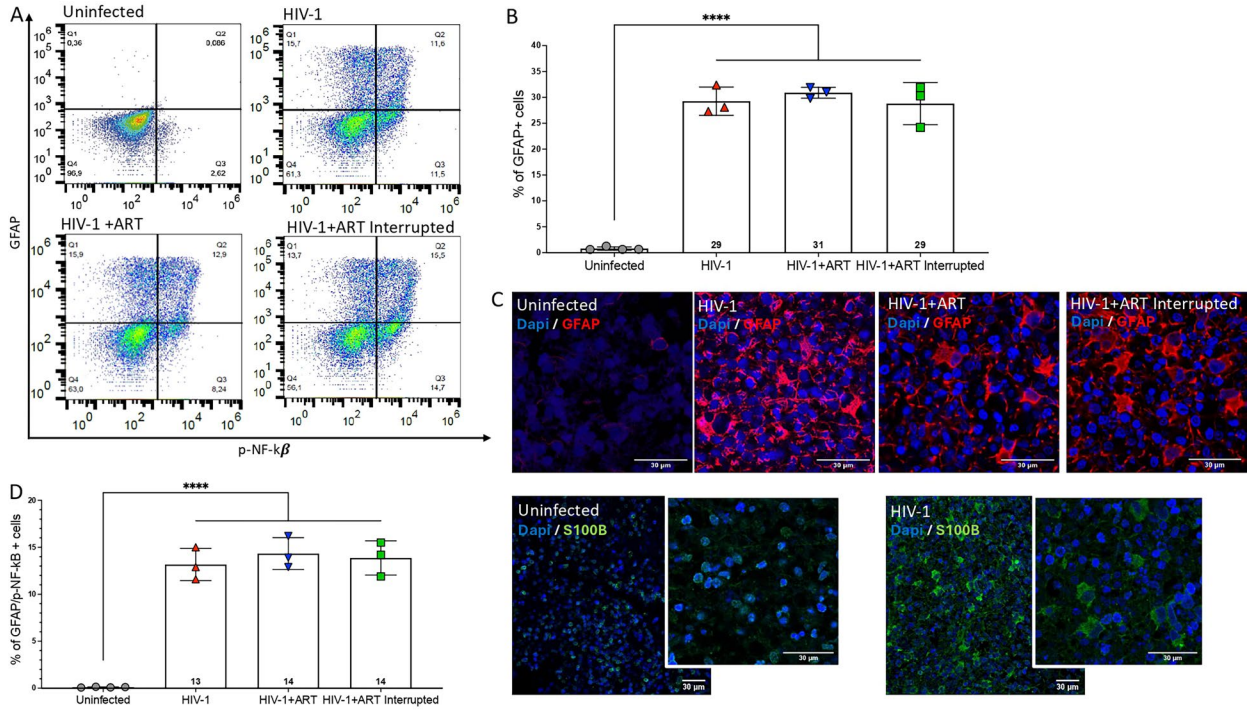

Fig. 3 HIV-1-infected microglia induce an increase in the reactive astrocyte population with elevated p-NF-kB levels. **A** Representative flow cytometry dot plot showing the population of reactive astrocyte (GFAP +) positive for p-NF-KB in M-BOs after 25 days of incubation in the four treatment conditions. **B** Graph quantifying the percentage of GFAP + cells in M-BOs in the four treatment conditions obtained by flow cytometry analysis. **C** Immunofluorescent staining for Dapi (blue) and GFAP (red) on slides of M-BOs in all conditions (top panels). Immunofluorescent staining for Dapi (blue) and S100B (green). Uninfected M-BOs vs HIV-1 M-Bos with an amplification from the same condition. **D** Graph quantifying the percentage of GFAP positive cells expressing p-NF-KB in M-BOs in the four treatment conditions obtained by flow cytometry analysis. Each organoid treated is an independent experiment and is represented by a single point in the graphs across for the four treatment conditions: Uninfected (n = 4), HIV-1 (n = 3), HIV-1 + ART (n = 3), and HIV-1 + ART Interrupted (n = 3). *p ≤ 0.05, **p ≤ 0.01, ***p ≤ 0.001,****p ≤ 0.0001

The neuroinflammation induced by HIV-1 infected microglia in BOs correlated with NF-kB activation of neurons in an ART-independent manner

Neurons are the primary cells affected in HIV-1-NCI, and postmortem tissue analysis from HIV-1-NCI shows that significant neuronal damage impacts their functions, viability and ultimately their survival [57, 58]. To assess how HIV-1 affected the percentage of neurons in the M-BO model, we used flow cytometry to analyze M-BOs in all four experimental conditions. The TUJ-1 marker revealed a consistent percentage of neurons in all conditions, with a notable increase in neuron population in the presence of ART (Fig. 4A and B) compared to the uninfected condition. To confirm this finding, we performed immunofluorescence using an additional marker for mature neurons (MAP2) and TUJ-1, both in combination with p-NF-kB. The images show representative samples for all conditions for MAP2. Although all conditions exhibited similar MAP2 expression, the marker intensity appears to be lower in the uninfected condition (Fig. 4C). The p-NF-kB signal appears stronger in the presence of HIV-1, though it is not distributed uniformly through the tissue.

Subsequent analysis of p-NF-kB levels in TUJ-1 positive cells by flow cytometry showed a significant increase in all infected conditions compared to uninfected (Fig. 4D). Remarkably, p-NF-kB levels did not respond to ART treatment, aligning with the pattern seen in microglia and astrocytes. This finding confirms that the neuronal population generates an inflammatory state due to interaction with HIV-1 infected microglia, which persists even under ART treatment. This aligns with features observed in individuals with HIV-1-NCI and suggests that HIV-1 infection combined with ART impacts neuron survival or neurogenesis in this in vitro model.

Neuroinflammation induced by HIV-1 infected microglia in BOs alters resident neural stem cell populations and NF-kB activation in an ART-dependent manner

The adult neurogenic process is regulated by many intrinsic and extrinsic factors [59]. Several studies have shown that HIV-1 can infect neuro-progenitor cells and

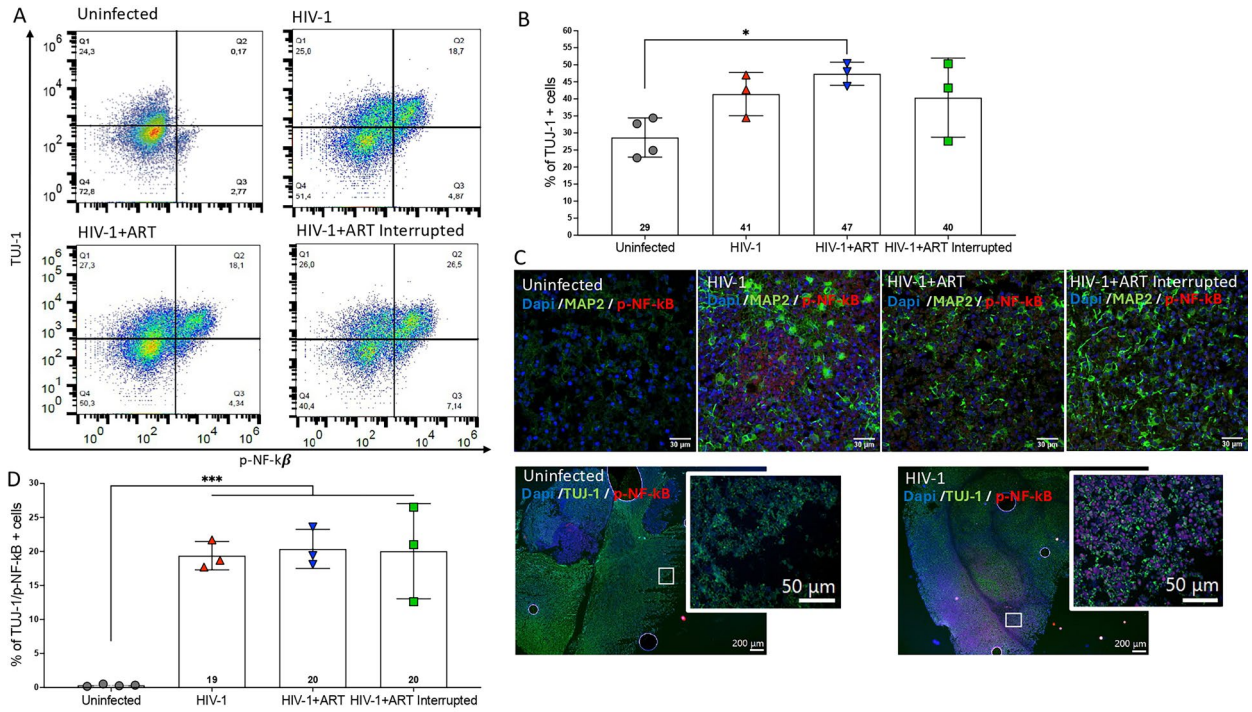

Fig. 4 HIV-1-infected microglia lead to an increase in p-NF-kB levels within the neuronal population. **A** Representative flow cytometry dot plot showing the population of Neurons (TUJ-1 positive cells) positive for p-NF-kB in M-BOs after 25 days of incubation for the four treatment conditions **B** Graph quantifying the percentage of TUJ-1 positive neurons in M-BOs for the four treatment conditions obtained by flow cytometry analysis **C** Immunofluorescent staining for Dapi (blue), MAP2 (green), and p-NF-KB (red) on slides of M-BOs for all conditions (top panels). Immunofluorescent staining for Dapi (blue), TUJ-1 (green), and p-NF-KB (red) on slides of Uninfected M-BOs vs HIV-1 M-BOs with an amplification of the indicated square area (bottom panels). **D** Graph quantifying the percentage of TUJ-1 positive neurons expressing p-NF-KB in M-BOs for the four treatment conditions obtained by flow cytometry analysis. Each organoid treated is an independent experiment and is represented by a single point in the graphs for the four treatment conditions: Uninfected (n = 4), HIV-1 (n = 3), HIV-1 + ART (n = 3), and HIV-1 + ART Interrupted (n = 3). *p ≤ 0.05, **p ≤ 0.01, ***p ≤ 0.001

affect neurogenesis [60, 61]. To evaluate the impact of HIV-1 infection and ART treatment on this population, we quantified neurons by flow cytometry and identified the population positive for PAX6 and SOX2. In the uninfected cultures, the double positive population was absent but was present in HIV-1-infected M-BOs (Fig. 5A). To corroborate this finding, we performed immunofluorescence using an additional NSC marker (Nestin). The images confirm a complete absence of the NSC population in the uninfected condition (Fig. 5B).

Interestingly, ART treatment seems to decrease the percentage of NSCs, but when ART was discontinued, the NSC population rebounded (Fig. 5C). This requires further study. The level of p-NF-kB was also evaluated in the NSC population (Fig. 5D). Among the NSCs from the M-BOs infected with HIV-1, the Mean Fluorescence Intensity (MFI) of p-NF-kB increased with ART treatment. We observed the shift in the MFI between HIV-1 M-BOs alone compared to HIV-1 + ART M-BOs in the representative histogram of p-NF-kB MFI (Fig. 5E).

Discussion

The use of in vitro models to study human neuropathology is critical to help better understand neuroinflammation and neuronal insults. In models of HIV-1 infection of the CNS, emerging evidence has demonstrated that BOs serve as a compelling model for studying neuropathology [38, 42, 43, 62], but with some limitations that we have addressed herein. One of the major limitations of brain BOs is their inability to fully recapitulate the complete repertoire of CNS cell types found in an adult brain. The absence of cells such as microglia and endothelial cells that form the Blood Brain Barrier as well as the presence of cells in an early developmental state, are important considerations in our analyses. Given that microglia are a primary reservoir of HIV-1, several studies have promoted the generation of microglia within the BOs or have introduced them exogenously to successfully replicate key aspects of HIV-1 neuropathogenesis [38, 42, 43, 62].

In this study, we added microglia exogenously and investigated the impact of HIV-1 infection, with or

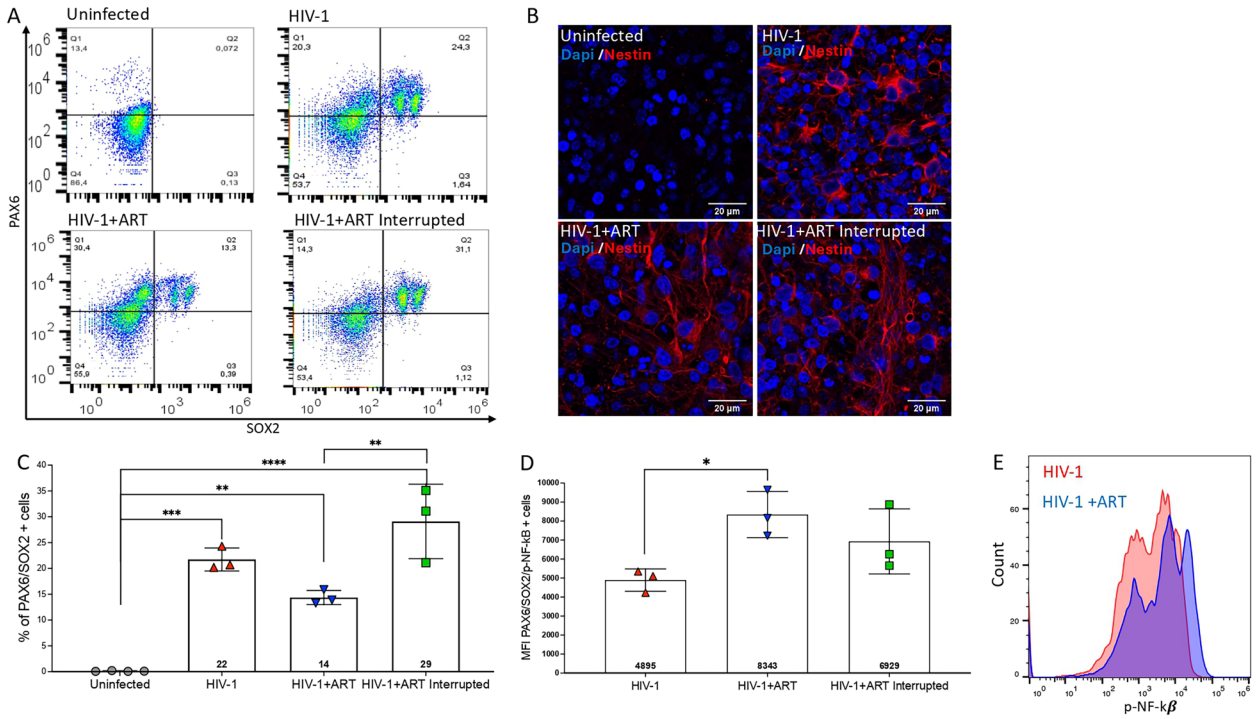

Fig. 5 The infiltration of HIV-1-infected microglia in BOs alters the neural stem cell population and p-NF-kB levels in an ART-dependent manner. **A** Representative flow cytometry dot plot of neural stem cell abundance, indicated by double positive signal for PAX6 and SOX2 in M-BOs for the four treatment conditions. **B** Immunofluorescent staining for Dapi (blue) and Nestin (red) for all conditions. **C** Graph quantifying the percentage of cells with a double positive signal for PAX6 and SOX2 in M-BOs for the four treatment conditions obtained by flow cytometry analysis. **D** Bar graph depicting the p-NF-kB MFI of cells double positive for PAX6 and SOX2 by flow cytometry analysis in M-BOs among the 3 experimental conditions: HIV-1, HIV-1 + ART, and HIV-1 + ART Interrupted. **E** Representative histogram showing p-NF-kB MFI of double positive population PAX6 and SOX2 of HIV-1 and HIV-1 + ART groups. Each organoid treated is an independent experiment and is represented by a single point in the graphs Uninfected (n = 4), HIV-1 (n = 3), HIV-1 + ART (n = 3), and HIV-1 + ART Interrupted (n = 3). *p ≤ 0.05, **p ≤ 0.01, ***p ≤ 0.001,****p ≤ 0.0001

without ART, on the neuroinflammatory process in the BOs.

HIV-1 infection generated an inflammatory response in the microglia, with expression of pro-inflammatory cytokines associated with HIV-1-NCI, including IL-1, IL-6, IL-10, IL-27, sCD163, sCD14, sTREM2 and OPN, by 3 days post-infection. The levels of sTREM2 in the supernatants of microglia cultures were higher after HIV-1 infection, suggesting receptor cleavage consistent with observations in people with HIV-1-NCI [21, 22]. This difference was noted even when only a few of the microglia were expressing TREM2 (22% in our flow cytometry analysis). The low level of TREM2 expression suggests heterogeneity during microglia differentiation that is also observed in human and mouse healthy adult brain, where the percentage of TREM2 express in microglia differs among brain regions [63, 64]. As TREM2 expression is known to be very dynamic, this heterogeneity is not unexpected [65].

Interestingly, the cytokine profile detected in the microglia supernatants differed from that detected in the supernatant of M-BOs. This suggests that the pro-inflammatory cytokines observed in BOs could have been contributed by various cell populations (astrocytes, neurons, NSCs), not just from microglia. These populations could be responding to primary inflammation initiated by microglia after infiltration, leading to the release of a distinct profile of pro-inflammatory cytokines.

The evaluation of HIV-1 infection in the model was tested by measuring the number of HIV-1 psi-gag copies integrated in the genome using ddPCR. HIV-1 psi-gag integration showed a high variability between the M-BOs. The high variation is also observed in other studies using exogenous microglia to model HIV-1-neuropathogenesis [38]. This could be a consequence of the variation in the infiltration of microglia into the BOs, or the size of the organoids. Additionally, ART treatment led to nearly undetectable p24, while without ART, p24 remained detectable. The p24 levels declined over time in all conditions, a trend also observed in a recent studies using BOs as model of HIV-1 that sustained replication with a similar timeframe [42]. However, despite the significant decrease in p24 levels in this model, neuroinflammatory markers (cytokines and p-NFKB levels) remained elevated until day 25, suggesting a model in which neuroinflammatory outcomes persist independently, post active HIV-1 replication. Previous studies have shown that healthy neurons can 'silence' HIV-1 in microglia when co-cultured together, preventing spontaneous reactivation from latency [40]. This suggests that active HIV-1 replication in microglia could enter into a transcriptionally inactive state in the presence of neuronal populations in the BOs. This will encourage further investigation into the latent state of HIV-1 in BOs, particularly since latency in microglia is interlinked with the inflammatory state of the local microenvironment [66].

The high p-NF-kB observed in the IBA-1 positive cells from the HIV-1 infected M-BOs suggest an inflammatory state that mimics one of the most significant characteristics of individuals with HIV-1-NCI-persistent neuroinflammation despite successful reduction in viral replication through ART [66, 67]. This was observed in the astrocyte population of our M-BOs, which showed a strong reactivation in HIV-1-infected M-BOs, independent of ART treatment, similar to that was observed with microglia. Although this has not yet been explored in the context of HIV-1 infection, studies have demonstrated that p65 p-NF-kB controls GFAP expression in neuroinflammatory diseases such as Alzheimer's disease [68]. While the exact relationship between these two molecules is still under investigation, both are clearly indicative of an astrogliosis state that may contribute significantly to the neuroinflammation in HIV-1 infection.

Proinflammatory cytokines remained high in the HIV-1 M-BO model. One of these cytokines is CCL2, one of the most classical cytokines associated with HIV-1-NCI [69, 70]. The main role of CCL2 in HIV-1-NCI is to recruit immune cells into the CNS, preferentially in to those cells that are infected [16–18]. In our model, CCL2 was the only cytokine that remained elevated throughout the entire experiment in all conditions where M-BOs were HIV-1 infected, including those treated with ART. These findings align with clinical observations of PLWH, who show sustained high levels of CCL2 in CSF even on ART [16, 71, 72].

Similarly, a recent HIV-1-NCI model utilizing BO under ART reported sustained CCL2 levels in the supernatant; however, this was only observed until day 9 of a 12-day incubation period [42]. In contrast, our model demonstrated persistently elevated CCL2 levels throughout the entire 25-day experiment, suggesting a more stable and prolonged representation of CCL2 over time. This provides a comparative advantage over other BO models. As such, our model serves as an ideal platform to study the role of CCL2 in neuro HIV-1 in the context of ART and its impact on the recruitment of peripheral immune cells, underscoring the need for further investigations that incorporate peripheral immune cells in to future studies.

Two cytokines associated with IRIS [23, 24], sCD14 and IL-27, were detected in the supernatant of M-BOs and had high levels of expression in HIV-1 M-BOs at the beginning and end of the study, respectively. However, contrary to our expectations for IRIS-associated cytokines, their levels were higher in the absence of ART,

suggesting that these cytokines may not be reliable markers for IRIS in our model.

Neurons could be damaged by the production of pro-inflammatory molecules as well as various HIV-1 viral proteins (such as Tat, gp120, and Rev) [73]. While the damage of neurons is commonly associated with cognitive impairment, little is known about the inflammation levels of neurons. A significant enhancement of p-NF-kB was observed in the TUJ-1 positive cells from the HIV-1-infected M-BOs that did not respond to ART treatment. A similar phenomenon was observed in NSCs. High p-NF-kB were detected in PAX6/SOX2 positive cells from HIV-1-infected M-BOs, which did not respond to ART treatment. This suggests that NSCs might also contribute to the pro-inflammatory state characteristic of HIV-1-NCI. Our data also shows a significant increase in the percentage of NSCs in HIV-1-infected conditions compared to uninfected conditions: a finding that contradicts some studies that suggest HIV-1 impairs neurogenesis [74–76]. However, it is known that during inflammation, inflammatory signals also positively influence neural cell proliferation, survival, migration, and differentiation [77]. For example, NF-kB can induce a conversion of mature astrocytes into neural progenitors [78]. Taken together, our results suggest that the neuroinflammation driven by HIV-1 could influence the maturation of glia cells impacting the progenitor reservoir. The effect of ART in this model, whereby the MFI of p-NF-kB in NSCs was higher in HIV-1 infected M-BOs treated with ART compared to other conditions, suggests that the combination of virus and ART elevates inflammation levels in the NSCs. Previous studies have shown that the combination of HIV-1 and ART induces varying degrees of oxidative stress and neuronal damage in the CNS, as shown by analyses of mitochondrial membrane potential [79–81].

The impact of ART in this model suggests that ART may potentially increase neuroinflammation. In a sizeable fraction of PLWH started on ART, excess inflammation manifests as IRIS, which can be a significant health risk [82]. While it seems intuitive that the in vivo immune system is largely responsible for this excess inflammation, it is possible that some effects of IRIS are driven by neuroinflammation, even in the absence of immune effectors. This M-BO model could help untangle non-immune events and virus driven CNS-IRIS events.

In our model, the sustained elevated levels of pro-inflammatory cytokines such as CCL2, which correlate with p-NF-KB levels in the presence of ART, establish this model as a reliable representation of HIV-1-NCI. Although the connection between p-NF-kB and CCL2 has been demonstrated in other pathological context [50–52], this is the first in vitro model of HIV-1 using BOs that links the clinical observations of high CCL2 levels found in the CSF of individuals with HIV-NCI undergoing ART [16, 71, 72] to increased p-NF-kB levels. In addition to the correlation observed through flow cytometry (p-NF-kB) and multiplex ELISA (CCL2), this was further supported by double-staining immunofluorescence for CCL2 and p-NF-kB, which revealed clusters of cells showing high levels of p-NF-kB alongside significant CCL2 presence. These findings encourage further research to understand the molecular mechanisms that render neuroinflammation, driven by these components, resistant to ART.

Conclusion

In this study, we established an in vitro model of HIV-1 with infected microglia to study the impact of HIV-1 and ART on inflammation in the CNS. We showed that infiltration of HIV-1 infected microglia into the BOs led to a proinflammatory state in astrocytes, neuronal, and NSC populations, that recapitulates some elements of neuroinflammation observed in HIV-1-NCI. ART failed to reverse neuroinflammation with continued elevated levels of cytokines such as CCL2 and OPN, and increased p-NF-kB, mirroring findings in individuals with HIV-1-NCI. This work develops an in vitro model of brain organoids that can be infected with HIV-1, and with this model, contributes to a better understanding of the persistent neuroinflammation observed in PLWH.

While further studies are needed to address the limitations of this model, it holds potential for identifying new therapeutic targets to treat neuroinflammation associated with HIV-1.

Abbreviations

HIV-1-NCI	HIV-1-associated neurocognitive impairment
PLWH	People Living with HIV
ART	Antiretroviral drug therapy
CNS	Nervous system
BOs	Cerebral brain organoids
IRIS	Immune Reconstitution Inflammatory Syndrome
CSF	Cerebrospinal fluid
CNS-IRIS	Nervous system Immune Reconstitution Inflammatory Syndrome CNS
NF-kB	Nuclear Factor kappa-light-chain-enhancer of activated B cells
p-NF-kB	Phospo-Nuclear Factor kappa-light-chain-enhancer of activated B cells
OPN	Osteopontin
sTREM	Soluble TREM2
IL	Interleukin
sCD163	Soluble CD163
IFNg	Interferon-gamma
TNFa	Tumor necrosis factor-alpha
sCD14	Soluble CD14
NSCs	Neuron stem cells
M-BO	Cerebral brain organoid infiltrated with microglia
ddPCR	Digital droplet PCR
ESCs	Embryonic stem cells

Supplementary Information

The online version contains supplementary material available at https://doi.org/10.1186/s12974-025-03375-w.

Supplementary Material 1.

Author contributions

SMM conceived, designed and performed experiments. SMM, DN, RFO, SM, STV and LN designed and analyzed experiments. TP and CF designed, performed and analyzed the Multiplex experiment. SC and HF produced in vitro cerebral organoids. SMM performed p24 ELISA, ddPCR, Immunofluorescence, differentiation of microglia, generation of M-BOs and flow cytometry. SMM, RFO, SM and DN wrote the manuscript. All authors read and approved the final manuscript.

Funding

This work resulted in part from research supported by National Institute on Drug Abuse (NIDA) award R01 DA052027, U01DA058527, and also in part by NIAID award number UM1AI164559 to LCN.

Availability of data and materials

No datasets were generated or analysed during the current study.

Declarations

Ethics approval and consent to participate

Not applicable.

Competing interests

The authors declare no competing interests.

Author details

[1]Institute of Translational Research, Feinstein Institutes for Medical Research, Northwell Health, Manhasset, NY, USA. [2]Division of Infectious Diseases, Department of Medicine, Weill Cornell Medicine, New York, NY, USA. [3]Meyer Cancer Center, Division of Neuro-Oncology, Department of Neurology, New York-Presbyterian Hospital/Weill Cornell Medicine, New York, NY, USA. [4]Department of Immunology and Microbiology, The Herbert Wertheim UF Scripps Institute for Biomedical Innovation and Technology, Jupiter, FL, USA.

Received: 20 July 2024 Accepted: 13 February 2025
Published online: 05 March 2025

References

1. Valcour V, Chalermchai T, Sailasuta N, et al. Central nervous system viral invasion and inflammation during acute HIV infection. J Infect Dis. 2012;206(2):275–82. https://doi.org/10.1093/infdis/jis326.
2. Wahl A, Al-Harthi L. HIV infection of non-classical cells in the brain. Retrovirology. 2023;20(1):1. https://doi.org/10.1186/s12977-023-00616-9.
3. Ash MK, Al-Harthi L, Schneider JR. HIV in the brain: identifying viral reservoirs and addressing the challenges of an HIV cure. Vaccines (Basel). 2021. https://doi.org/10.3390/vaccines9080867.
4. Kolson DL. Developments in neuroprotection for HIV-associated neurocognitive disorders (HAND). Curr HIV/AIDS Rep. 2022;19(5):344–57. https://doi.org/10.1007/s11904-022-00612-2.
5. Chen P-P, Wei X-Y, Tao L, Xin X, Xiao S-T, He N. Cerebral abnormalities in HIV-infected individuals with neurocognitive impairment revealed by fMRI. Sci Rep. 2023;13(1):10331. https://doi.org/10.1038/s41598-023-37493-3.
6. Scanlan A, Zhang Z, Koneru R, et al. A rationale and approach to the development of specific treatments for HIV associated neurocognitive impairment. Microorganisms. 2022. https://doi.org/10.3390/microorganisms10112244.
7. Alford K, Daley S, Banerjee S, Vera JH. Quality of life in people living with HIV-associated neurocognitive disorder: a scoping review study. PLoS ONE. 2021;16(5): e0251944. https://doi.org/10.1371/journal.pone.0251944.
8. Nightingale S, Ances B, Cinque P, et al. Cognitive impairment in people living with HIV: consensus recommendations for a new approach. Nat Rev Neurol. 2023;19(7):424–33. https://doi.org/10.1038/s41582-023-00813-2.
9. Elendu C, Aguocha CM, Okeke CV, Okoro CB, Peterson JC. HIV-related neurocognitive disorders: diagnosis, treatment, and mental health implications: a review. Medicine (Baltimore). 2023;102(43): e35652. https://doi.org/10.1097/md.0000000000035652.
10. Heaton RK, Clifford DB, Franklin DR Jr, et al. HIV-associated neurocognitive disorders persist in the era of potent antiretroviral therapy: CHARTER Study. Neurology. 2010;75(23):2087–96. https://doi.org/10.1212/WNL.0b013e318200d727.
11. Li Q, Barres BA. Microglia and macrophages in brain homeostasis and disease. Nat Rev Immunol. 2018;18(4):225–42. https://doi.org/10.1038/nri.2017.125.
12. Cosenza MA, Zhao ML, Si Q, Lee SC. Human brain parenchymal microglia express CD14 and CD45 and are productively infected by HIV-1 in HIV-1 encephalitis. Brain Pathol. 2002;12(4):442–55. https://doi.org/10.1111/j.1750-3639.2002.tb00461.x.
13. Wallet C, De Rovere M, Van Assche J, et al. Microglial cells: the main HIV-1 reservoir in the brain. Front Cell Infect Microbiol. 2019;9:362. https://doi.org/10.3389/fcimb.2019.00362.
14. Schlachetzki JCM, Zhou Y, Glass CK. Human microglia phenotypes in the brain associated with HIV infection. Curr Opin Neurobiol. 2022;77: 102637. https://doi.org/10.1016/j.conb.2022.102637.
15. Borrajo López A, Penedo MA, Rivera-Baltanas T, et al. Microglia: the real foe in HIV-1-associated neurocognitive disorders? Biomedicines. 2021. https://doi.org/10.3390/biomedicines9080925.
16. Kim B-H, Hadas E, Kelschenbach J, et al. CCL2 is required for initiation but not persistence of HIV infection mediated neurocognitive disease in mice. Sci Rep. 2023;13(1):6577. https://doi.org/10.1038/s41598-023-33491-7.
17. Hernandez C, Gorska AM, Eugenin E. Mechanisms of HIV-mediated blood-brain barrier compromise and leukocyte transmigration under the current antiretroviral era. iScience. 2024;27(3): 109236. https://doi.org/10.1016/j.isci.2024.109236.
18. Eugenin EA, Osiecki K, Lopez L, Goldstein H, Calderon TM, Berman JW. CCL2/monocyte chemoattractant protein-1 mediates enhanced transmigration of human immunodeficiency virus (HIV)-infected leukocytes across the blood-brain barrier: a potential mechanism of HIV–CNS invasion and neuroAIDS. J Neurosci. 2006;26(4):1098–106. https://doi.org/10.1523/jneurosci.3863-05.2006.
19. Brown A, Islam T, Adams R, et al. Osteopontin enhances HIV replication and is increased in the brain and cerebrospinal fluid of HIV-infected individuals. J Neurovirol. 2011;17(4):382–92. https://doi.org/10.1007/s13365-011-0035-4.
20. Mahmud FJ, Du Y, Greif E, et al. Osteopontin/secreted phosphoprotein-1 behaves as a molecular brake regulating the neuroinflammatory response to chronic viral infection. J Neuroinflamm. 2020;17(1):273. https://doi.org/10.1186/s12974-020-01949-4.
21. Gisslén M, Heslegrave A, Veleva E, et al. CSF concentrations of soluble TREM2 as a marker of microglial activation in HIV-1 infection. Neurol Neuroimmunol Neuroinflamm. 2019;6(1): e512. https://doi.org/10.1212/nxi.0000000000000512.
22. Fields JA, Spencer B, Swinton M, et al. Alterations in brain TREM2 and Amyloid-β levels are associated with neurocognitive impairment in HIV-infected persons on antiretroviral therapy. J Neurochem. 2018;147(6):784–802. https://doi.org/10.1111/jnc.14582.
23. Vinhaes CL, Sheikh V, Oliveira-de-Souza D, et al. an inflammatory composite score predicts mycobacterial immune reconstitution inflammatory syndrome in people with advanced HIV: a prospective international cohort study. J Infect Dis. 2021;223(7):1275–83. https://doi.org/10.1093/infdis/jiaa484.
24. Musselwhite LW, Andrade BB, Ellenberg SS, et al. Vitamin D, D-dimer, interferon γ, and sCD14 levels are independently associated with immune reconstitution inflammatory syndrome: a prospective, international study. EBioMedicine. 2016;4:115–23. https://doi.org/10.1016/j.ebiom.2016.01.016.

25. Wong CS, Richards ES, Pei L, Sereti I. Immune reconstitution inflammatory syndrome in HIV infection: taking the bad with the good. Oral Dis. 2017;23(7):822–7. https://doi.org/10.1111/odi.12606.
26. Bahr N, Boulware DR, Marais S, Scriven J, Wilkinson RJ, Meintjes G. Central nervous system immune reconstitution inflammatory syndrome. Curr Infect Dis Rep. 2013;15(6):583–93. https://doi.org/10.1007/s11908-013-0378-5.
27. Liu T, Zhang L, Joo D, Sun S-C. NF-κB signaling in inflammation. Signal Transduct Target Ther. 2017;2(1):17023. https://doi.org/10.1038/sigtrans.2017.23.
28. Lawrence T. The nuclear factor NF-kappaB pathway in inflammation. Cold Spring Harb Perspect Biol. 2009;1(6): a001651. https://doi.org/10.1101/cshperspect.a001651.
29. Zhang Q, Lenardo MJ, Baltimore D. 30 Years of NF-κB: a blossoming of relevance to human pathobiology. Cell. 2017;168(1–2):37–57. https://doi.org/10.1016/j.cell.2016.12.012.
30. Anilkumar S, Wright-Jin E. NF-κB as an inducible regulator of inflammation in the central nervous system. Cells. 2024. https://doi.org/10.3390/cells13060485.
31. Shih RH, Wang CY, Yang CM. NF-kappaB signaling pathways in neurological inflammation: a mini review. Front Mol Neurosci. 2015;8:77. https://doi.org/10.3389/fnmol.2015.00077.
32. Sullivan PG, Bruce-Keller AJ, Rabchevsky AG, et al. Exacerbation of damage and altered NF-kappaB activation in mice lacking tumor necrosis factor receptors after traumatic brain injury. J Neurosci. 1999;19(15):6248–56. https://doi.org/10.1523/jneurosci.19-15-06248.1999.
33. Laruelle M. Imaging synaptic neurotransmission with in vivo binding competition techniques: a critical review. J Cereb Blood Flow Metab. 2000;20(3):423–51. https://doi.org/10.1097/00004647-200003000-00001.
34. Jiang G, Dandekar S. Targeting NF-κB signaling with protein kinase C agonists as an emerging strategy for combating HIV latency. AIDS Res Hum Retroviruses. 2015;31(1):4–12. https://doi.org/10.1089/aid.2014.0199.
35. Rostasy K, Monti L, Yiannoutsos C, et al. NFkappaB activation, TNF-alpha expression, and apoptosis in the AIDS-Dementia-Complex. J Neurovirol. 2000;6(6):537–43. https://doi.org/10.3109/13550280009091954.
36. Hatziioannou T, Evans DT. Animal models for HIV/AIDS research. Nat Rev Microbiol. 2012;10(12):852–67. https://doi.org/10.1038/nrmicro2911.
37. Eichmüller OL, Knoblich JA. Human cerebral organoids—a new tool for clinical neurology research. Nat Rev Neurol. 2022;18(11):661–80. https://doi.org/10.1038/s41582-022-00723-9.
38. Dos Reis RS, Sant S, Keeney H, Wagner MCE, Ayyavoo V. Modeling HIV-1 neuropathogenesis using three-dimensional human brain organoids (hBORGs) with HIV-1 infected microglia. Sci Rep. 2020;10(1):15209. https://doi.org/10.1038/s41598-020-72214-0.
39. Zhang W, Jiang J, Xu Z, et al. Microglia-containing human brain organoids for the study of brain development and pathology. Mol Psychiatry. 2023;28(1):96–107. https://doi.org/10.1038/s41380-022-01892-1.
40. Alvarez-Carbonell D, Ye F, Ramanath N, et al. Cross-talk between microglia and neurons regulates HIV latency. PLoS Pathog. 2019;15(12): e1008249. https://doi.org/10.1371/journal.ppat.1008249.
41. Ryan SK, Gonzalez MV, Garifallou JP, et al. Neuroinflammation and EIF2 signaling persist despite antiretroviral treatment in an hiPSC Tri-culture model of HIV infection. Stem Cell Rep. 2020;14(4):703–16. https://doi.org/10.1016/j.stemcr.2020.02.010.
42. Kong W, Frouard J, Xie G, et al. Neuroinflammation generated by HIV-infected microglia promotes dysfunction and death of neurons in human brain organoids. PNAS Nexus. 2024. https://doi.org/10.1093/pnasnexus/pgae179.
43. Donadoni M, Cakir S, Bellizzi A, Swingler M, Sariyer IK. Modeling HIV-1 infection and neuroHIV in hiPSCs-derived cerebral organoid cultures. J Neurovirol. 2024. https://doi.org/10.1007/s13365-024-01204-z.
44. Lancaster MA, Renner M, Martin CA, et al. Cerebral organoids model human brain development and microcephaly. Nature. 2013;501(7467):373–9. https://doi.org/10.1038/nature12517.
45. Linkous A, Balamatsias D, Snuderl M, et al. Modeling patient-derived glioblastoma with cerebral organoids. Cell Rep. 2019;26(12):3203-3211.e5. https://doi.org/10.1016/j.celrep.2019.02.063.
46. Wilson PG, Stice SS. Development and differentiation of neural rosettes derived from human embryonic stem cells. Stem Cell Rev. 2006;2(1):67–77. https://doi.org/10.1007/s12015-006-0011-1.
47. Sabate-Soler S, Nickels SL, Saraiva C, et al. Microglia integration into human midbrain organoids leads to increased neuronal maturation and functionality. Glia. 2022;70(7):1267–88. https://doi.org/10.1002/glia.24167.
48. Zicari S, Sessa L, Cotugno N, et al. Immune activation, inflammation, and non-AIDS co-morbidities in HIV-infected patients under long-term ART. Viruses. 2019. https://doi.org/10.3390/v11030200.
49. Burdo TH, Weiffenbach A, Woods SP, Letendre S, Ellis RJ, Williams KC. Elevated sCD163 in plasma but not cerebrospinal fluid is a marker of neurocognitive impairment in HIV infection. AIDS. 2013;27(9):1387–95. https://doi.org/10.1097/QAD.0b013e32836010bd.
50. Deng X, Xu M, Yuan C, et al. Transcriptional regulation of increased CCL2 expression in pulmonary fibrosis involves nuclear factor-κB and activator protein-1. Int J Biochem Cell Biol. 2013;45(7):1366–76. https://doi.org/10.1016/j.biocel.2013.04.003.
51. Nakatsumi H, Matsumoto M, Nakayama KI. Noncanonical pathway for regulation of CCL2 expression by an mTORC1-FOXK1 axis promotes recruitment of tumor-associated macrophages. Cell Rep. 2017;21(9):2471–86. https://doi.org/10.1016/j.celrep.2017.11.014.
52. Khorooshi R, Babcock AA, Owens T. NF-kappaB-driven STAT2 and CCL2 expression in astrocytes in response to brain injury. J Immunol. 2008;181(10):7284–91. https://doi.org/10.4049/jimmunol.181.10.7284.
53. Patani R, Hardingham GE, Liddelow SA. Functional roles of reactive astrocytes in neuroinflammation and neurodegeneration. Nat Rev Neurol. 2023;19(7):395–409. https://doi.org/10.1038/s41582-023-00822-1.
54. Sabri F, Titanji K, De Milito A, Chiodi F. Astrocyte activation and apoptosis: their roles in the neuropathology of HIV infection. Brain Pathol. 2003;13(1):84–94. https://doi.org/10.1111/j.1750-3639.2003.tb00009.x.
55. Liu X, Bae C, Gelman B, Chung JM, Tang S-J. Mechanism and role of astrogliosis in the pathogenesis of HIV-associated pain one sentence summary: neuron-to-astrocyte Wnt5a signaling-activated astrogliosis is essential for the development of pathological pain induced by HIV-1 gp120. bioRxiv 2021:2021.04.28.441838. https://doi.org/10.1101/2021.04.28.441838.
56. Valdebenito S, Castellano P, Ajasin D, Eugenin EA. Astrocytes are HIV reservoirs in the brain: a cell type with poor HIV infectivity and replication but efficient cell-to-cell viral transfer. J Neurochem. 2021;158(2):429–43. https://doi.org/10.1111/jnc.15336.
57. Williams ME, Naudé PJW. The relationship between HIV-1 neuroinflammation, neurocognitive impairment and encephalitis pathology: a systematic review of studies investigating post-mortem brain tissue. Rev Med Virol. 2024;34(1): e2519. https://doi.org/10.1002/rmv.2519.
58. Mattson MP, Haughey NJ, Nath A. Cell death in HIV dementia. Cell Death Differ. 2005;12(1):893–904. https://doi.org/10.1038/sj.cdd.4401577.
59. Lu C, Garipler G, Dai C, et al. Essential transcription factors for induced neuron differentiation. Nat Commun. 2023;14(1):8362. https://doi.org/10.1038/s41467-023-43602-7.
60. Putatunda R, Ho WZ, Hu W. HIV-1 and compromised adult neurogenesis: emerging evidence for a new paradigm of HAND persistence. AIDS Rev. 2019;21(1):11–22. https://doi.org/10.24875/AIDSRev.19000003.
61. Lawrence DM, Durham LC, Schwartz L, Seth P, Maric D, Major EO. Human immunodeficiency virus type 1 infection of human brain-derived progenitor cells. J Virol. 2004;78(14):7319–28. https://doi.org/10.1128/jvi.78.14.7319-7328.2004.
62. Dos Reis RS, Sant S, Ayyavoo V. Three-dimensional human brain organoids to model HIV-1 neuropathogenesis. Methods Mol Biol. 2023;2610:167–78. https://doi.org/10.1007/978-1-0716-2895-9_14.
63. Schmid CD, Sautkulis LN, Danielson PE, et al. Heterogeneous expression of the triggering receptor expressed on myeloid cells-2 on adult murine microglia. J Neurochem. 2002;83(6):1309–20. https://doi.org/10.1046/j.1471-4159.2002.01243.x.
64. Qu W, Li L. Microglial TREM2 at the intersection of brain aging and Alzheimer's disease. Neuroscientist. 2023;29(3):302–16. https://doi.org/10.1177/10738584211040786.
65. Liu W, Taso O, Wang R, et al. Trem2 promotes anti-inflammatory responses in microglia and is suppressed under pro-inflammatory conditions. Hum Mol Genet. 2020;29(19):3224–48. https://doi.org/10.1093/hmg/ddaa209.
66. Sreeram S, Ye F, Garcia-Mesa Y, et al. The potential role of HIV-1 latency in promoting neuroinflammation and HIV-1-associated neurocognitive disorder. Trends Immunol. 2022;43(8):630–9. https://doi.org/10.1016/j.it.2022.06.003.

67. Bai R, Li Z, Lv S, et al. Persistent inflammation and non-AIDS comorbidities during ART: coming of the age of monocytes. Front Immunol. 2022;13: 820480. https://doi.org/10.3389/fimmu.2022.820480.
68. Jong Huat T, Camats-Perna J, Newcombe EA, et al. The impact of astrocytic NF-κB on healthy and Alzheimer's disease brains. Sci Rep. 2024;14(1):14305. https://doi.org/10.1038/s41598-024-65248-1.
69. Packard TA, Schwarzer R, Herzig E, et al. CCL2: a chemokine potentially promoting early seeding of the latent HIV reservoir. MBio. 2022;13(5): e0189122. https://doi.org/10.1128/mbio.01891-22.
70. Ansari AW, Heiken H, Meyer-Olson D, Schmidt RE. CCL2: a potential prognostic marker and target of anti-inflammatory strategy in HIV/AIDS pathogenesis. Eur J Immunol. 2011;41(12):3412–8. https://doi.org/10.1002/eji.201141676.
71. Christo PP, Vilela MdC, Bretas TL, et al. Cerebrospinal fluid levels of chemokines in HIV infected patients with and without opportunistic infection of the central nervous system. J Neurol Sci. 2009;287(1):79–83. https://doi.org/10.1016/j.jns.2009.09.002.
72. Cinque P, Vago L, Ceresa D, et al. Cerebrospinal fluid HIV-1 RNA levels: correlation with HIV encephalitis. AIDS. 1998;12(4):389–94. https://doi.org/10.1097/00002030-199804000-00007.
73. Kovalevich J, Langford D. Neuronal toxicity in HIV CNS disease. Future Virol. 2012;7(7):687–98. https://doi.org/10.2217/fvl.12.57.
74. Krathwohl MD, Kaiser JL. HIV-1 promotes quiescence in human neural progenitor cells. J Infect Dis. 2004;190(2):216–26. https://doi.org/10.1086/422008.
75. Ferrell D, Giunta B. The impact of HIV-1 on neurogenesis: implications for HAND. Cell Mol Life Sci. 2014;71(22):4387–92. https://doi.org/10.1007/s00018-014-1702-4.
76. Fan Y, Gao X, Chen J, Liu Y, He JJ. HIV tat impairs neurogenesis through functioning as a notch ligand and activation of notch signaling pathway. J Neurosci. 2016;36(44):11362–73. https://doi.org/10.1523/jneurosci.1208-16.2016.
77. Kizil C, Kyritsis N, Brand M. Effects of inflammation on stem cells: together they strive? EMBO Rep. 2015;16(4):416–26. https://doi.org/10.15252/embr.201439702.
78. Gabel S, Koncina E, Dorban G, et al. Inflammation promotes a conversion of astrocytes into neural progenitor cells via NF-κB activation. Mol Neurobiol. 2016;53(8):5041–55. https://doi.org/10.1007/s12035-015-9428-3.
79. Akay C, Cooper M, Odeleye A, et al. Antiretroviral drugs induce oxidative stress and neuronal damage in the central nervous system. J Neurovirol. 2014;20(1):39–53. https://doi.org/10.1007/s13365-013-0227-1.
80. Stern AL, Lee RN, Panvelker N, et al. Differential effects of antiretroviral drugs on neurons in vitro: roles for oxidative stress and integrated stress response. J Neuroimmune Pharmacol. 2018;13(1):64–76. https://doi.org/10.1007/s11481-017-9761-6.
81. Robertson K, Liner J, Meeker RB. Antiretroviral neurotoxicity. J Neurovirol. 2012;18(5):388–99. https://doi.org/10.1007/s13365-012-0120-3.
82. Haddow LJ, Moosa MY, Mosam A, Moodley P, Parboosing R, Easterbrook PJ. Incidence, clinical spectrum, risk factors and impact of HIV-associated immune reconstitution inflammatory syndrome in South Africa. PLoS ONE. 2012;7(11): e40623. https://doi.org/10.1371/journal.pone.0040623.
83. Festa L, Gutoskey CJ, Graziano A, Waterhouse BD, Meucci O. Induction of Interleukin-1β by Human Immunodeficiency Virus-1 Viral Proteins Leads to Increased Levels of Neuronal Ferritin Heavy Chain, Synaptic Injury, and Deficits in Flexible Attention. J Neurosci. 2015;35(29):10550–61. https://doi.org/10.1523/jneurosci.4403-14.2015.
84. Brabers NA, Nottet HS. Role of the pro-inflammatory cytokines TNF-alpha and IL-1beta in HIV-associated dementia. Eur J Clin Invest. 2006;36(7):447–58. https://doi.org/10.1111/j.1365-2362.2006.01657.x.
85. Schrier RD, Hong S, Crescini M, et al. Cerebrospinal fluid (CSF) CD8+ T-cells that express interferongamma contribute to HIV associated neurocognitive disorders (HAND). PLoS One. 2015;10(2):526. https://doi.org/10.1371/journal.pone.0116526.
86. Li W, Henderson LJ, Major EO, Al-Harthi L. IFN-gamma mediates enhancement of HIV replication in astrocytes by inducing an antagonist of the betacatenin pathway (DKK1) in a STAT 3-dependent manner. J Immunol. 2011;186(12):6771–8. https://doi.org/10.4049/jimmunol.1100099.
87. Liu X, Kumar A. Differential signaling mechanism for HIV-1 Nef-mediated production of IL-6 and IL-8 in human astrocytes. Sci Reports. 2015;5(1):9867. https://doi.org/10.1038/srep09867.
88. Argandona Lopez C, Brown AM. Microglial- neuronal crosstalk in chronic viral infection through mTOR, SPP1/OPN and inflammasome pathway signaling. Front Immunol. 2024;15:1368465. https://doi.org/10.3389/fimmu.2024.1368465.
89. Sénécal V, Barat C, Gagnon MT, et al. Altered expression of fractalkine in HIV-1-infected astrocytes and consequences for the virus-related neurotoxicity. J Neurovirol. 2021;27(2):279–301. https://doi.org/10.1007/s13365-021-00955-3.
90. Mudra Rakshasa-Loots A, Whalley HC, Vera JH. Cox SR Neuroinflammation in HIV-associated depression: evidence and future perspectives. Molecular Sychiatry. 2022;27(9):3619–32. https://doi.org/10.1038/s41380-022-01619-2.
91. Saleh S, Lu HK, Evans V, et al. HIV integration and the establishment of latency in CCL19-treatedresting CD4(+) T cells require activation of NF-κB. Retrovirology. 2016;13(1):49. https://doi.org/10.1186/s12977-016-0284-7.
92. Mo L, Su G, Su H, Huang W, Luo X, Tao C. Effect of IL-10 in the pathogenesis of HIV/AIDS patients with cryptococcal meningitis. Mol Cell Biochem. 2023;478(1):1–11. https://doi.org/10.1007/s11010-022-04488-z.

Publisher's Note